General and Comparative Endocrinology 278 (2019) 58–67

Contents lists available at ScienceDirect

General and Comparative Endocrinology

journal homepage: www.elsevier.com/locate/ygcen

Evaluation of Aib and PEG-polymer insect kinin analogs on mosquito and tick GPCRs identifies potent new pest management tools with potentially enhanced biostability and bioavailability

Caixing Xiong[a], Krzysztof Kaczmarek[b,c], Janusz Zabrocki[b,c], Patricia V. Pietrantonio[a,*], Ronald J. Nachman[b,*]

[a] Department of Entomology, Texas A&M University, College Station, TX 77843, USA
[b] Insect Control and Cotton Disease Research Unit, Southern Plains Agricultural Research Center, U.S. Department of Agriculture, 2881 F/B Road, College Station, TX 77845, USA
[c] Institute of Organic Chemistry, Lodz University of Technology, 90-924 Lodz, Poland

ARTICLE INFO

Keywords:
Leucokinin
Aedes aegypti
Rhipicephalus microplus
Cattle fever tick
Arthropod disease vectors
Calcium bioluminescence assay

ABSTRACT

Insect kinins modulate aspects of diuresis, digestion, development, and sugar taste perception in tarsi and labellar sensilla in mosquitoes. They are, however, subject to rapid biological degradation by endogenous invertebrate peptidases. A series of α-aminoisobutyric (Aib) acid-containing insect kinin analogs incorporating sequences native to the *Aedes aegypti* mosquito aedeskinins were evaluated on two recombinant kinin invertebrate receptors stably expressed in cell lines, discovering a number of highly potent and biostable insect kinin mimics. On the *Ae. aegypti* mosquito kinin receptor, three highly potent, biostable Aib analogs matched the activity of the Aib-containing biostable insect kinin analog 1728, which previously showed disruptive and/or aversive activity in aphid, mosquito and kissing bug. These three analogs are IK-Aib-19 ([Aib]FY[Aib]WGa, EC_{50} = 18 nM), IK-Aib-12 (pQKFY[Aib]WGa, EC_{50} = 23 nM) and IK-Aib-20 ([Aib]FH[Aib]WGa, EC_{50} = 28 nM). On the *Rhipicephalus (Boophilus) microplus* tick receptor, IK-Aib-20 ([Aib]FH[Aib]WGa, EC_{50} = 2 nM) is more potent than 1728 by a factor of 3. Seven other potentially biostable analogs exhibited an EC_{50} range of 5–10 nM, all of which match the potency of 1728. Among the multi-Aib hexapeptide kinin analogs tested the tick receptor has a preference for the positively-charged, aromatic H over the aromatic residues Y and F in the X^1 variable position ([Aib]FX^1[Aib]WGa), whereas the mosquito receptor does not distinguish between them. In contrast, in a mono-Aib pentapeptide analog framework (FX^1[Aib]WGa), both receptors exhibit a preference for Y over H in the variable position. Among analogs incorporating polyethylene glycol (PEG) polymer attachments at the N-terminus that can confer enhanced bioavailability and biostability, three matched or surpassed the potency of a positive control peptide. On the tick receptor IK-PEG-9 (P_8-R[Aib]FF[Aib]WGa) was the most potent. Two others, IK-PEG-8 (P_8-RFFPWGa) and IK-PEG-6 (P_4-RFFPWGa), were most potent on the mosquito receptor, with the first surpassing the activity of the positive control peptide. These analogs and others in the IK-Aib series expand the toolbox of potent analogs accessible to invertebrate endocrinologists studying the structural requirements for bioactivity and the as yet unknown role of the insect kinins in ticks. They may contribute to the development of selective, environmentally friendly pest arthropod control agents.

1. Introduction

Insect neuropeptides of the insect kinin (IK) class regulate important biological functions in invertebrates (Coast, 2007; Coast et al., 2002; De Loof, 2008; Gäde, 2004; Nässel, 2002). In diverse species insect kinins stimulate hindgut contractions, diuresis, digestive enzyme release, probably inhibit lepidopteran larval weight gain, participate in tracheal clearance and air filling prior to ecdysis in *Drosophila*, and modulate sugar taste perception in contact chemosensory neurons in *Ae. aegypti* mosquitoes (Coast et al., 1990; Harshini et al., 2003; Holman et al., 1990; Kersch and Pietrantonio, 2011; Kim et al., 2018; Kwon et al., 2016; Lu et al., 2011a; Nachman et al., 2002; Pietrantonio et al., 2005; Seinsche et al., 2000).

Neuropeptides have been studied as potential leads for the

* Corresponding authors.
E-mail addresses: p-pietrantonio@tamu.edu (P.V. Pietrantonio), nachman@tamu.edu (R.J. Nachman).

https://doi.org/10.1016/j.ygcen.2018.08.002
Received 24 May 2018; Received in revised form 2 July 2018; Accepted 1 August 2018
Available online 11 August 2018
0016-6480/ Published by Elsevier Inc.

development of new, environmentally friendly pest control agents due to their specificity and high activity at very low doses. However, the natural peptides cannot be directly used, as they are susceptible to degradation by endogenous peptidases (Cornell et al., 1995; Gäde and Goldsworthy, 2003; Lamango et al., 1996; Nachman et al., 2002). In addition, they are not suitably designed to penetrate the exoskeleton of invertebrate pests. Knowledge of both chemical and conformational requirements responsible for neuropeptide biological activity can aid in the design of analogs containing unnatural moieties that can overcome these limitations (Nachman et al., 1994).

The endogenous arthropod insect kinins are 6–14 amino acid long neuropeptides characterized by the evolutionarily conserved C-terminal pentapeptide Phe-X^1-X^2-Trp-Gly-NH_2, where X^1 = His, Asn, Ser, or Tyr and X^2 = Ser, Pro, or Ala (Holman et al., 1999; Torfs et al., 1999). This C-terminal pentapeptide kinin core is the minimum sequence required for full cockroach myotropic and cricket diuretic activity in tissue assays *in vitro* (Nachman et al., 2003; Nachman and Holman, 1991). Recombinant kinin receptors from the southern cattle tick, *Rhipicephalus* (*Boophilus) microplus* (Holmes et al., 2003; Holmes et al., 2000) and the dengue vector, the mosquito *Aedes aegypti* (Pietrantonio et al., 2005) were previously stably expressed in CHO-K1 cells for comparative structure-activity relationship studies of kinin analogs. This assay system confirmed the activity of the kinin pentapeptide core in both receptors (Holmes et al., 2003; Pietrantonio et al., 2005; Taneja-Bageshwar et al., 2006). Both the tissue assays and the receptor expressing system revealed that the C-terminal amide of the insect kinins is important for their activity (Nachman et al., 1995; Taneja-Bageshwar et al., 2006). Activity was also lost when either Phe^1 or Trp^4 was replaced with Ala, confirming the importance of these two key positions (Taneja-Bageshwar et al., 2006). However, the variable position 2 tolerates a wide range of chemical characteristics, from acidic to basic residues, and from hydrophilic to hydrophobic, although highest potencies were observed with aromatic residues at this position (Nachman and Holman, 1991; Roberts et al., 1997; Taneja-Bageshwar et al., 2006). Based on these observations the plausible receptor interaction model positions the side chains of Phe^1 and Trp^4 towards the same region via a β-turn involving the Pro^3 where they interact with the receptor, and away from the side chain of position 2.

Insect kinins are subject to rapid degradation by peptidases present in the haemolymph and bound to tissues of invertebrate pests. The primary hydrolysis-susceptible site lies within the insect kinin C-terminal pentapeptide core region between the Ser^3 (or Pro^3) and conserved Trp^4 residues. A secondary site is found just outside of the core region at the peptide bond N-terminal to Phe^1. Experimentally, the fly angiotensin converting enzyme (ACE) can cleave the insect kinin primary hydrolysis site, and neprilysin (NEP) can cleave both the primary and secondary hydrolysis sites (Cornell et al., 1995; Lamango et al., 1996; Nachman et al., 1997a; Nachman et al., 1997b; Nachman et al., 1990; Nachman et al., 2002; Roberts et al., 1997). Replacement of Ser^3 (or Pro^3) with an unnatural, sterically bulky residue Aib leads to analogs that not only mimic a critical β-turn conformation but also blocks tissue-bound peptidase, ANCE, and NEP hydrolysis, with FF[Aib]WGa maintaining potency in mosquito and tick recombinant receptors (Nachman et al., 1997a; Nachman et al., 1997b; Nässel, 2002; Taneja-Bageshwar et al., 2009; Taneja-Bageshwar et al., 2006). Incorporation of a second Aib residue adjacent to the secondary peptidase hydrolysis site further enhances biostability (Nachman et al., 2002). The disubstituted Aib kinin analog [Aib]FS[Aib]WGa was resistant to enzymatic degradation up to 4 h (Nachman et al., 2002). Analog 1728, [Aib]FF[Aib]WGa (also referred to as K-Aib-1), and related to the aforementioned multi-Aib analog, does not contain residues specific to the native aedeskinins apart from the C-terminal pentapeptide FX^1X^2WGa that is conserved in invertebrate kinins. It was several fold (from 300 to 20) less susceptible to hydrolysis by a number of these enzymes as compared with the insect kinin FFFSWGa (Taneja-Bageshwar et al., 2009). The resistance to aminopeptidase hydrolysis is likely due to the steric hindrance of the α,α-disubstituted nature of the amino acid Aib located at the N-terminus. In both tick and mosquito kinin receptor expressing cell lines, analog 1728 was more potent than the positive control (FFFSWGa) and aedeskinin 2 (Taneja-Bageshwar et al., 2009). The N-terminus of FF[Aib]WGa is still vulnerable to hydrolysis by aminopeptidases. This analog is less potent than the aedeskinins (up to 14 residues in length), as the mosquito receptor prefers sequences extended beyond the C-terminal pentapeptide core (Taneja-Bageshwar et al., 2009; Taneja-Bageshwar et al., 2008; Taneja-Bageshwar et al., 2006). Extended insect kinin analogs would also require additional protection from peptidases that attack at the secondary site.

We now continued the design of pseudopeptides with enhanced resistance to peptidases that retain biological activity on 'insect kinin' receptors of arthropod vectors in search of analogs with higher potency, biostability and bioavailability. In this paper, we develop a new series of kinin analog pest management tools by further exploring the use of the sterically-hindered Aib moiety in biostable analogs that also specifically incorporate residues from insect kinins native to the mosquito *Aedes aegypti*, aedeskinin-1, -2 and -3 (Predel et al., 1997; Veenstra et al., 1997). In a few of these analogs the N-terminus is further protected from aminopeptidases with either acetyl (Ac-) or pyroglutamate (pQ-) groups (Nachman et al., 2002).

Another approach to the stabilization of peptides and/or proteins to enzymatic degradation in the digestive system as well as the enhancement of penetration across cell membranes of the gut or cuticle into the hemolymph (blood) of insects is the conjugation of polyethylene glycol (PEG) polymers (Fig. 1) to the N-terminus (Boccù et al., 1982; Jeffers and Roe, 2008; Shen et al., 2009). Although not previously applied to neuropeptides of the insect kinin class, conjugation of PEG polymers to the insect peptide trypsin modulating oostatic factor (TMOF) enhanced the resistance to degradation by the digestive enzyme leucine aminopeptidase, leading to accumulation of the peptide in hemolymph of insects and ticks (Boccù et al., 1982; Jeffers and Roe, 2008; Shen et al., 2009). Five insect kinin analogs incorporating PEG_4 (P_4) and PEG_8 (P_8) polymers (Fig. 1) at the N-terminus, three of which also incorporate the sterically-hindered Aib residue were evaluated in this study on the two recombinant invertebrate 'insect kinin' receptors. We have determined their potency (EC_{50}), their efficacy in comparison to a kinin analog serving as positive control (FFFSWGa) and correlated these two variables to rank these analogs.

2. Materials and methods

2.1. Analog synthesis and purification

Analogs were synthesized on an ABI 433A peptide synthesizer with a modified FastMoc 0.25 procedure using an Fmoc-strategy starting from Rink amide resin (Novabiochem, San Diego, CA, 0.5 mM/g). The Fmoc protecting group was removed by 20% 4-methyl piperidine in DMF (Dimethyl formamide). A fourfold excess of the respective Fmoc-amino acids was activated *in situ* using HBTU (2-(1 h-benzotriazol-1-yl)-1,1,3,3-tetramethyluronium hexafluorophosphate) (1 eq.)/HOBt (1-

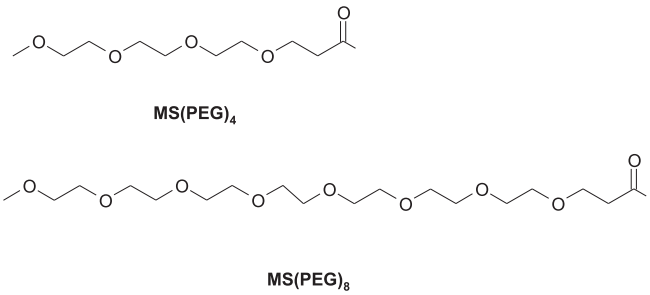

Fig. 1. Structures of P4 and P8 attached to the N-terminus of the IK-PEG analogs.

hydroxybenzotriazole) (1 eq.) in NMP (N-methylpyrrolidone) or HATU (2-(7-Aza-1H-Benzotiazole-1-yl)-1,1,3,3-tetramethyluronium hexafluorophosphate) (1 eq.)/HOAt (1-hydroxy-7-azabenzotriazole) (1 eq.) in NMP for Aib and the amino acid immediately following it in the sequence. The coupling reactions were base catalyzed with DIPEA (N,N-diisopropylethylamine) (4 eq.) The amino acid side chain protecting groups were PMC for Arginine and Boc for Tryptophan. Acetylation was accomplished as previously described (Taneja-Bageshwar et al., 2009).

The PEG polymer conjugations were accomplished as follows: after transferring peptidyl resin with the completed peptide sequence into an 8 ml polypropylene syringe, a 1.2 M equivalent of MS(PEG_4) or MS(PEG_8) reagent was added as a 10% solution in NMP (100 mg of viscous reagent was reconstituted with 900 mg NMP). Both reagents are commercially available (Thermo Scientific, Waltham, MA) and they are N-hydroxysuccinimide esters of O-methyl-tetra- and octa-ethyleneglycolcarboxylic acid, respectively. The syringes were shaken over night at RT and, following a positive Kaiser test, EDC was added (0.5 eq.) and shaken for one additional day. After washing with DCM (3×) and methanol (3×) and drying the PEGylated peptide analogs, cleavage from the resin was accomplished with a cocktail composed of TFA/DMB/TIS (92.5:5:2.5), and precipitated with ether.

The analogs were cleaved from the resin with side-chain deprotection by treatment with TFA (Trifluoroacetic acid):H_2O:TIS (Triisopropylsilane) (95.5:2.5:2.5 v/v/v) for 1.5 h. The solvents were evaporated by vacuum centrifugation and the analogs were desalted on a Waters C_{18} Sep Pak cartridge (Milford, MA) in preparation for purification by HPLC.

The analogs were purified on a Waters Delta-Pak C_{18} reverse-phase column (8 × 100 mm, 15 μm particle size, 100 Å pore size) with a Waters 510 HPLC system with detection at 214 nm at ambient temperature. Solvent A = 0.1% aqueous trifluoroacetic acid (TFA); Solvent B = 80% aqueous acetonitrile containing 0.1% TFA. Initial conditions were 10% B followed by a linear increase to 90% B over 40 min; flow rate, 2 ml/min. Delta-Pak C_{18} retention times: **IK-Aib-5**, Ac-FF[Aib]WGa, 4.5 min; **IK-PEG-6**, MS[PEG_4]-RFFPWGa, 10.5 min; **IK-Aib-7**, MS[PEG_4]-R[Aib]FF[Aib]WGa, 12.0 min; **IK-PEG-8**, MS[PEG_8]-RFFPWGa, 9.0 min; **IK-PEG-9**, MS[PEG_8]-R[Aib]FH[Aib]WGa, 12.0 min; **IK-PEG-10**, MS[PEG_8]-[Aib]FH[Aib]WGa, 12.5 min; **IK-Aib-11**, NSKYVSKQKFY[Aib]WGa, 2.5 min; **IK-Aib-12**, pQKFY[Aib]WGa, 2.3 min; **IK-Aib-13**, NPFH[Aib]WGa, 2.4 min; **IK-Aib-14**, Ac-FH[Aib]WGa, 2.4 min; **IK-Aib-15**, FH[Aib]WGa, 2.3 min; **IK-Aib-16**, FY[Aib]WGa, 2.3 min; **IK-Aib-17**, VFY[Aib]WGa, 2.5 min; **IK-Aib-18**, pQVFY[Aib]WGa, 6.6 min; **IK-Aib-19**, [Aib]FY[Aib]WGa, 2.3 min; **IK-Aib-20**, [Aib]FH[Aib]WGa, 2.5 min. The analogs were further purified on a Waters Protein Pak I 125 column (7.8 x 300 mm). Conditions: isocratic using 80% acetonitrile containing 0.1% TFA; flow rate, 2 ml/min. Waters Protein Pak retention times: **IK-Aib-5**, 5.9 min; **IK-PEG-6**, 6.0 min; **IK-PEG-7**, 6.0 min; **IK-PEG-8**, 6.25 min; **IK-PEG-9**, 5.9 min; **IK-PEG-10**, 4.75 min; **IK-Aib-11**, 9.25 min; **IK-Aib-12**, 6.25 min; **IK-Aib-13**, 7.0 min; **IK-Aib-14**, 6.25 min; **IK-Aib-15**, 6.25 min; **IK-Aib-16**, 6.0 min; **IK-Aib-17**, 6.0 min; **IK-Aib-18**, 6.0 min; **IK-Aib-19**, 6.0 min; **IK-Aib-20**, 6.25 min. Amino acid analysis was carried out under previously reported conditions (Nachman et al., 2004) to quantify the analogs and to confirm identity: **IK-Aib-5**: F[2.0], G[0.9]; **IK-PEG-6**: F[2.0], G[0.9]; P[1.0]; R[1.1]; **IK-PEG-7**: F[2.0], G[0.9], R[1.0]; **IK-PEG-8**: F[2.0], G[0.9], R[1.0]; **IK-PEG-9**: F[2.0], G[0.9], R[0.8]; **IK-PEG-10**: F[2.0], G[0.9]; **IK-Aib-11**: E[1.0]; F[1.0], G[0.9], K[2.7]; N[0.9]; S[0.9]; V[0.9]; Y[2.0]; **IK-Aib-12**: E[1.1]; F[1.1], G[1.0]; K[1.1]; P[1.0]; R[1.1], Y[1.2]; **IK-Aib-13**: D[1.0]; F[1.0], G[1.0]; H[1.0]; **IK-Aib-14**: F[1.0], G[1.1]; H[1.0]; **IK-Aib-15**: F[1.0], G[1.1]; H[1.0]; **IK-Aib-16**: F[1.0], G[1.0]; Y[1.2]; **IK-Aib-17**: F[1.0], G[1.1]; V[0.9]; Y[1.2]; **IK-Aib-18**: E[1.1]; F[1.0], G[1.0]; V[1.0]; Y[1.1]; **IK-Aib-19**: F[1.0], G[1.0]; Y[1.1]; **IK-Aib-20**: F[1.0], G[1.1]; H[0.9]. The identity of the analogs was also confirmed by MALDI-MS on a Kratos Kompact Probe MALDI-MS instrument (Shimadzu, Columbia, Maryland). The following molecular ions (MH^+) were observed: **IK-Aib-5**, 704.7 (calc.704.5 [MNa^+]); **IK-PEG-6**, 1027.3 (1027.5 calc.); **IK-PEG-7**, 1100.2 (1100.2 calc.); **IK-PEG-8**, 1203.7 (1203.4 calc.); **IK-PEG-9**, 1276.9 (1276.4 calc.); **IK-PEG-10**, 1120.0 (1120.3 calc.); **IK-Aib-11**, 1719.2 (1719.0 calc.); **IK-Aib-12**, 895.4 (895.0 calc.); **IK-Aib-13**, 841.7 (841.0 calc.); **IK-Aib-14**, 673.3 (673.0 calc.); **IK-Aib-15**, 630.4 (630.0 calc.); **IK-Aib-16**, 656.3 (656.0 calc.); **IK-Aib-17**, 755.3 (755.0 calc.); **IK-Aib-18**, 866.0 (866.0 calc.); **IK-Aib-19**, 741.1 (740.0 calc.); **IK-Aib-20**, 715.4 (715.0 calc.).

2.2. Cell lines

BMLK3 and IGKN F10 are CHO-K1 cell lines stably expressing the cattle fever tick (*Rhipicephalus microplus* (Canestrini)) and yellow fever mosquito (*Aedes aegypti* L.) kinin receptors, respectively. Receptor cloning, transfection and selection of single clonal cell lines expressing these kinin receptors were reported previously (Holmes et al., 2003; Pietrantonio et al., 2005). A cell line similarly transfected with empty vector plasmid pcDNA3.1 (Invitrogen) was designated “vector-only” (V/O) and used as negative control in all experiments. Cells were maintained in T-25 flasks (CELLSTAR®, Greiner Bio-one) with maintenance medium consisting of F-12K medium (Corning™ cellgro™, Mediatech, Inc. VA, US), fetal bovine serum (FBS) (10%) (Equitech-Bio, Kerrville, TX) and 400 μg/ml G418 Sulfate (Gibco™, New York, US). Cells were maintained in a humidified incubator at 37 °C, 5% CO_2. Unless specified otherwise, cells were incubated under these conditions.

2.3. Analysis of activity of kinin analogs by a calcium-mobilization bioluminescence assay

Kinin receptors of both *R. microplus* and *A. aegypti* couple to G_q protein, and its signaling cascade triggers calcium release from intracellular calcium stores (Holmes et al., 2003; Pietrantonio et al., 2005). The functional analyses of kinin analogs with stably transformed CHO-K1 cells expressing the tick and mosquito receptor was performed by an intracellular calcium mobilization bioluminescence assay. This assay was described in detail elsewhere (Lu et al., 2011b) and uses the calcium reporter aequorin. In brief, receptor-expressing cell lines and V/O cell line maintained in T-25 flasks were cultured to about 90% confluency, and were then trypsinized. The cells were suspended in maintenance medium, counted and diluted to 1×10^5 cells/ml; 2 ml of this cell suspension were placed into each well of 6-well-plates (CELLSTAR®, Greiner Bio-one). After overnight incubation, when the cells reached a confluency of 40–60%, old medium was replaced with 1 ml of serum-reduced Opti-MEM™ medium (Gibco™, New York, US) in each well. Following the instructions of the transfection reagent manufacturer, cells in each well of 6-well plate were transiently transfected with 1 μg mtAequorin/pcDNA1 plasmid mixed in 4 μl of FuGENE6 (Promega, Madison, WI) and 96 μl of Opti-MEM™ medium. After 6 h of incubation, the old medium was then replaced with 2 ml of F-12 K medium with FBS (10%) (antibiotic-free medium). Following 24 h incubation, cells were trypsinized and seeded into white-wall clear-bottom 96-well-plates (CELLSTAR® 655098, Greiner Bio-one) at 20,000 cell/well in 100 μl of antibiotic-free medium, and incubated overnight until cells reached confluency of 80%. To reconstitute the aequorin-complex, cells were incubated with 90 μl per well of calcium-free DMEM (1×) (Gibco®, Invitrogen) containing coelenterazine (5 μM) (Regis® Technology, Inc., Morton Grove, IL). After 3 h of incubation in the dark, cells were ready for the assay. The assays were performed with a Clariostar™ (BMG Labtechnology, Chicago, IL) plate reader set at 29 °C for bioluminescence and well-mode at 469 nm emission wavelength.

2.4. Determination of agonist activity of peptidomimetics

To determine whether kinin analogs behave as agonists on the kinin receptors and to avoid wasting the valuable custom-synthesized peptides, all 16 analogs were initially screened at 1 μM; only analogs that

showed agonist activity (determined by *t*-test comparison with cells injected with blank medium, preliminary data not shown) were chosen to continue testing in concentration-response analyses (IK-AIB-10 did not show activity on mosquito receptor; not shown).

Dose-dependent tests were performed on the 16 new kinin analogs as well as other two insect kinin receptor agonists, FFFSWGa and 1728 ([Aib]FF[Aib]WGa), (Taneja-Bageshwar et al., 2009) for comparison purposes. Dry peptides were solubilized, and serially diluted in calcium-free DMEM medium containing 1% Dimethyl sulfoxide (DMSO) and prepared as 10x stock. Each analog was tested with both receptor cell lines, at each of 9 concentrations from 0.1 nM to 10 μM. For this, cells in wells in 90 μl of DMEM medium were challenged with 10 μl of 10× concentration of potential agonist injected into the wells at a speed of 430 μl/s, for a final volume of 100 μl in the wells. Immediately after the injection, calcium mobilization-dependent bioluminescence was recorded for 30 s at 2 s interval, as the signal usually diminished within 30 s. In each assay, each concentration was tested in duplicate wells for each receptor cell line and at least two wells of each of the following controls were included: 1) V/O cell line as negative control; 2) DMSO (1%) in DMEM (blank medium) injected to cells as background injection controls for each cell line, and 3) FFFSWGa at 1 μM was injected as positive control (PC). Three independent replicates were performed for all analogs except for analog 1728 (n = 2).

2.5. Data analysis

In each well, the response of cells to a stimulus was calculated by averaging bioluminescence units elicited during 30 s, that is, as readout, the area under the bioluminescence vs. time response curve was chosen. The response for each replicate was represented as the average of responses from the two pseudo-replicate wells for each concentration, and for each control. For analyses, the background cellular response to blank medium injection was subtracted from the cellular responses to analogs.

All statistical analyses and graphs were done with GraphPad Prism 6.0 (GraphPad Software, La Jolla, CA). For calculations of EC_{50s} these values were then normalized to the maximal response (100%) observed among all concentrations tested for each analog. EC_{50} was defined as the concentration that elicited 50% of the highest number of bioluminescence units for that analog (100%). Dose-response curves (Suppl. Fig. 1), estimated EC_{50} values, and their respective 95% confidence intervals were calculated with "non-linear regression log[agonist] vs. normalized (bioluminescence) response" with "variable slope function". One-way ANOVA was performed to compare potency (log.EC_{50}) of active analogs, followed by Tukey multiple comparison test (Suppl. Tables 1.1 and 2.1).

The bioluminescence response of the PC at 1 μM (100%) in each assay plate was used to normalize the bioluminescence dose-response curves of all analogs. These curves were generated by "non-linear regression log[agonist] vs. response" with variable slope (four parameters). The efficacy was calculated as percentage of the bioluminescence response of each analog at 1 μM with reference to the bioluminescence response of the PC at 1 μM (100%). The 1 μM concentration was chosen to calculate efficacy because most analog responses plateaued at this concentration and analogs that required higher concentrations were not considered as an improvement over PC, and for this reason were of lesser interest. One-way ANOVA was performed on efficacy of each of the active analog at 1 μM followed by Tukey multiple comparison test (Suppl. Tables 1.2 and 2.2).

Correlation analyses between the Log.EC_{50} of each analog (Table 1) and the efficacy (Table 2) were performed. The Pearson correlation (two-tailed) analysis was done independently for the tick and mosquito receptor data sets. The linear regression lines and the 95% confidence intervals (dashed lines) were calculated with "Best-fit value" setting using GraphPad Prism 6.0 (GraphPad Software, La Jolla, CA). The analyses aided the discrimination and visualization of groups of analogs with high potency and high efficacy (Fig. 3). For both receptors, analogs with efficacy above that of the PC was desirable. For activity on the mosquito receptor, an $EC_{50} < 100$ nM was desirable, and for tick receptor, an $EC_{50} < 10$ nM.

Table 1
Novel biostable kinin analogs incorporating aedeskinin sequences, Aib or PEG.

Aib analogs incorporating the aedeskinin 1 sequence NSKYVSKQKFY**S**WGa:	
IK-Aib-11	NSKYVSKQKFY[Aib]WGa
IK-Aib-12	pQKFY[Aib]WGa
Aib analogs incorporating the aedeskinin 3 sequence NNPNVFYPWGa:	
IK-Aib-18	pQVFY[Aib]WGa
IK-Aib-17	VFY[Aib]WGa
Aib analogs incorporating aedeskinin 1 and 3 sequences (both end in FYXWGa; X = P or S):	
IK-Aib-16	FY[Aib]WGa
IK-Aib-19	[Aib]FY[Aib]WGa
IK-Aib-5	Ac-FF[Aib]WGa
Aib analogs incorporating the aedeskinin 2 sequence NPFHAWGa:	
IK-Aib-13	NPFH[Aib]WGa
IK-Aib-14	Ac-FH[Aib]WGa
IK-Aib-15	FH[Aib]WGa
IK-Aib-20	[Aib]FH[Aib]WGa
Analogs incorporating either PEG_4 [MS(PEG_4)] or PEG_8 [MS(PEG_8)] polymer attachments (Fig. 1):	
IK-PEG-6	P_4-RFFPWGa
IK-PEG-8	P_8-RFFPWGa
IK-PEG-7	MS(PEG_4)-R[Aib]FF[Aib]WGa
IK-PEG-9	MS(PEG_8)-R[Aib]FF[Aib]WGa
IK-PEG-10	MS(PEG_8)-[Aib]FF[Aib]WGa

IK stands for Insect Kinin analog, Aib represents α-aminoisobutyric acid and PEG is an abbreviation for polyethylene glycol polymer.

3. Results and discussion

A total of sixteen novel insect kinin (IK) analogs (Table 1) were evaluated in both tick and mosquito receptors in an aequorin-based intracellular calcium functional assay. The goal was to extend the number of biostable and highly potent IK analog tools available to endocrinologists studying the role of the IKs and their potential application in pest management strategies. All analogs were compared to a positive control (PC) peptide FFFSWGa without modifications, and to a potent Aib analog, 1728 previously characterized (Fig. 2; Suppl. Fig. 1). The efficacy was calculated as the ratio of bioluminescence responses of analogs to that of the PC, when all peptides were applied at 1 μM (Table 2). This concentration was chosen because most analogs elicited their maximal response (plateau) at 1 μM (Fig. 2), dosages beyond 1 μM would not be considered an improvement over already developed analogs. The normalization of responses to 1 μM (100%) was necessary for comparative purposes of analog responses within tick or mosquito receptor tests (Fig. 2).

Statistical analyses run independently for EC_{50} (Suppl. Tables 1.1 and 2.1) and efficacy (Suppl. Tables 1.2 and 2.2) did not always allow a clear ranking of analogs. Therefore, the two variables EC_{50} and the efficacy were subjected to correlation analyses, and based on these results analogs were classified into groups (Fig. 3). For both receptors there was a strong positive correlation between efficacy and potency, each with $P < 0.0001$ and $R^2 > 0.7$. In sum, a more potent analog (lower EC_{50}) tended to show a higher efficacy (responded with a higher number of bioluminescence units) (Fig. 3). For both receptors, (EC_{50}) (Table 2) of the analogs could be separated into three groups with significantly higher EC_{50} than the PC (Suppl. Tables 1.1 and 2.1). For the mosquito receptor: group *a* had increased potency by at least a factor of 14, group *b* had increased potency by a factor of 5–8, and group *c*, which exhibited increased potency by a factor of 3–4. For the tick receptor: group *a*, had increased potency by a factor of 8, group *b* had increased potency by a factor of 4–6, and group *c* (IK-Aib-15) by a factor of 3.

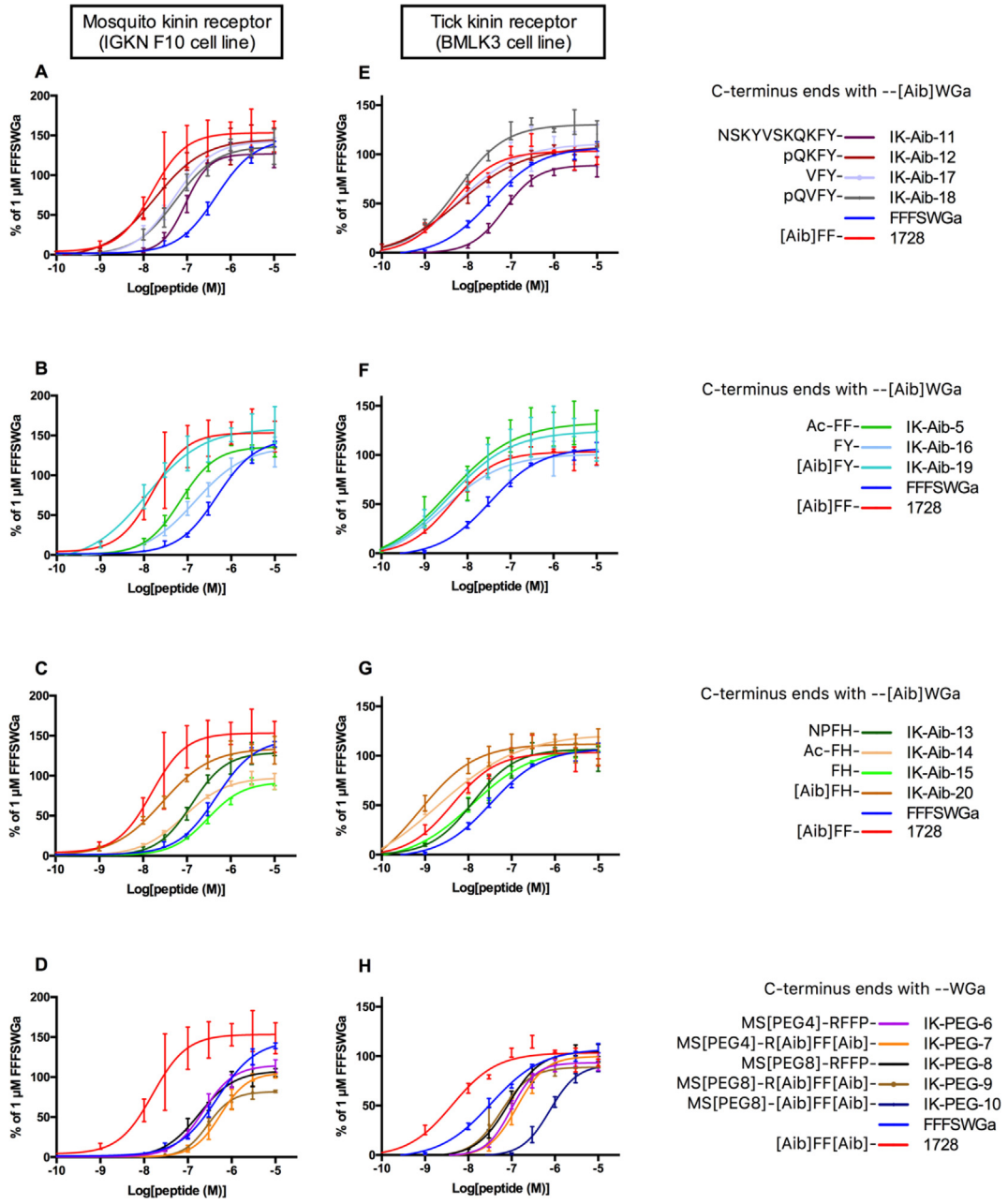

Fig. 2. Dose-dependent bioluminescence responses of IK analogs relative to the bioluminescence response elicited by 1 µM of the positive control peptide FFFSWGa. Mosquito (A-D) and tick (E-H) recombinant kinin receptors expressed in CHO-K1 cells were tested against 17- and 18- insect kinin analogs, respectively, each at 9 concentrations from 10^{-10} to 10^{-5} M (Log on X-axis) using a calcium bioluminescence assay (the IK-PEG-10 analog was not active on mosquito receptor). The Y-axis (Mean ± SEM) represents the percentage of bioluminescence response (average bioluminescence units elicited during 30 s) of each analog concentration in reference to the bioluminescence response elicited by 1 µM of positive control analog, FFFSWGa (100%). This peptide was included in each plate for each analog test for normalization. Three replicates were performed for all analogs except for analog 1728 (n = 2). Dose-response curves were generated with non-linear regression log(agonist) vs. response – variable slope (four parameters) function with GraphPad Prism 6.0 (GraphPad Software, La Jolla, CA). Each figure showed receptor responses to a group of analogs of similar design; their complete sequence is shown in Table 1. The panel figure legend highlights analogs' features. A) and E): endogenous sequence of either aedeskinin-1 or -3. B) and F): endogenous sequence of both aedeskinin-1 and -3. C) and G): endogenous sequence of aedeskinin-2. D) and H): polyethylene glycol (PEG) modified. The dose-response curves for FFFSWGa (positive control) and 1728 ([Aib]FF[Aib]WGa, a potent [Aib] agonist) were included in each figure for comparison.

3.1. Novel insect kinin Aib analog design

A new series of eleven biostable, Aib-containing IK analogs incorporated the sequence of the three native aedeskinins neuropeptides of the mosquito *Ae. aegypti* (Table 1). One group of six IK analogs featured incorporation of the sequences of aedeskinin 1, aedeskinin 3 or both, and share the same Y residue in the variable 2nd position of the C-terminal pentapeptide FYXWGa (Table 1). In aedeskinin 1, the variable position X is occupied by an S, whereas in aedeskinin 3 it is occupied by a P; though the distinction is inconsequential because in this analog series the position is occupied by Aib. Analog IK-Aib-11 (NSKYVSKQFY [Aib]WGa) features an Aib residue imbedded into the turn region of the entire sequence of aedeskinin 1 (Table 1). Analogs IK-Aib-19, IK-Aib-5 and IK-Aib-16 are not only analogs of aedeskinin 1, but also of aedeskinin 3. The aedeskinin 2 series shares a histidine (H) in the variable position. Analog IK-Aib-13 features an Aib imbedded in the entire

Table 2
Estimated potencies (EC_{50}) of insect kinin (IK) analogs on recombinant mosquito (IGKNF 10) and tick (BMLK3) receptors.

Rank of EC_{50}[1]	IK Sequence	Name	EC_{50} (nM)	95% Confidence Interval (nM)	Efficacy (%)[2]	SEM of efficacy (%; n=3)
Mosquito receptor (IGKNF10 cell line)						
1[a]	[Aib]FF[Aib]WGa	1728	17.16	11.85-26.17	152.98	9.89
2[a]	[Aib]FY[Aib]WGa	IK-Aib-19	18.17	13.14-24.64	150.70	2.86
3[a]	pQKFY[Aib]WGa	IK-Aib-12	23.23	17.68-30.52	136.12	18.86
4[a]	[Aib]FH[Aib]WGa	IK-Aib-20	28.32	21.58-37.18	132.25	8.71
5[b]	VFY[Aib]WGa	IK-Aib-17	52.63	43.51-63.66	133.07	2.65
6[b]	pQVFY[Aib]WGa	IK-Aib-18	77.12	55.03-108.1	138.07	2.69
7[b]	Ac-FF[Aib]WGa	IK-Aiib-5	78.37	55.19-114.3	144.35	5.92
8[d]	Ac-FH[Aib]WGa	IK-Aib-14	83.88	69.33-101.5	90.17	2.85
9[c]	NSKYVSKQKFY[Aib]WGa	IK-Aib-11	109.6	84.44-142.1	130.16	9.04
10[c]	FY[Aib]WGa	IK-Aib-16	132.3	112.5-155.6	110.84	5.79
11[c]	NPFH[Aib]WGa	IK-Aib-13	151.1	128.1-178.4	114.10	2.51
12[e]	MS[PEG8]-RFFPWGa	IK-PEG-8	181.8	154.8-213.5	97.29	4.55
13[e]	MS[PEG4]-RFFPWGa	IK-PEG-6	240.4	210.4-274.6	94.92	6.52
14[e]	MS[PEG8]-R[Aib]FF[Aib]WGa	IK-PEG-9	308.1	271.7-349.3	68.78	4.01
15[e]	FH[Aib]WGa	IK-Aib-15	310.8	254.4-382.6	67.85	2.79
16[e]	FFFSWGa	PC	398.1	345.6-458.5	100.00	0.00
17[e]	MS[PEG4]-R[Aib]FF[Aib]WGa	IK-PEG-7	505.7	457.4-558.9	72.05	10.53
18[*]	MS[PEG8]-[Aib]FF[Aib]WGa	IK-PEG-10	-	-	1.08	-
Tick receptor (BMLK3 cell line)						
1[a]	[Aib]FH[Aib]WGa	IK-Aib-20	2.091	1.350-3.239	111.74	4.24
2[a]	Ac-FH[Aib]WGa	IK-Aib-14	5.024	3.623-6.967	113.95	1.02
3[a]	FY[Aib]WGa	IK-Aib-16	5.176	3.358-7.978	112.23	10.12
4[b]	[Aib]FF[Aib]WGa	1728	6.612	3.275-13.35	104.80	0.85
5[b]	Ac-FF[Aib]WGa	IK-Aib-5	6.192	4.540-10.52	137.09	5.48
6[b]	pQVFY[Aib]WGa	IK-Aib-18	8.240	5.014-13.54	124.41	1.78
7[b]	pQKFY[Aib]WGa	IK-Aib-12	8.630	6.092-12.23	104.88	0.77
8[b]	[Aib]FY[Aib]WGa	IK-Aib-19	9.561	5.478-16.70	128.91	3.75
9[b]	VFY[Aib]WGa	IK-Aib-17	9.925	7.027-14.02	108.07	1.84
10[c]	FH[Aib]WGa	IK-Aib-15	15.17	11.05-20.28	101.49	0.89
11[c]	NPFH[Aib]WGa	IK-Aib-13	18.08	10.71-27.24	111.19	2.73
12[d]	FFFSWGa	PC	41.01	33.63-50.01	100.00	0.00
13[d]	MS[PEG8]-R[Aib]FF[Aib]WGa	IK-PEG-9	61.90	51.19-74.85	85.30	2.58
14[d]	MS[PEG8]-RFFPWGa	IK-PEG-8	93.41	82.14-106.2	95.35	1.26
15[d]	NSKYVSKQKFY[Aib]WGa	IK-Aib-11	106.6	72.57-156.6	81.92	2.79
16[d]	MS[PEG4]-RFFPWGa	IK-PEG-6	108.0	92.17-126.7	90.27	4.90
17[d]	MS[PEG4]-R[Aib]FF[Aib]WGa	IK-PEG-7	160.2	127.5-201.2	90.36	5.17
18[e]	MS[PEG8]-[Aib]FF[Aib]WGa	IK-PEG-10	758.5	666.1-863.8	53.71	4.43

[a–e]Different groups of analogs were categorized based on their agonist activities from high (a) to low (e) on each receptor, and by potency (EC_{50}) and efficacy. See correlation of potency and efficacy (Fig. 3).
[1] EC_{50} values: concentration that elicited 50% of the highest number of bioluminescence units for that analog (100%); n = 3 (except for 1728, n = 2). Analogs are ranked by EC_{50} from more potent to less potent.
[2] Efficacy was calculated as percentage of the bioluminescence response of each analog tested at 1 μM concentration, with reference to the bioluminescence response elicited by 1 μM of analog FFFSWGa (PC).
* IK-PEG-10: no activity on mosquito receptor at 1 μM; it was not further tested.

sequence of aedeskinin 2; whereas IK-Aib-15, IK-Aib-14 and IK-Aib-20 are fragment analogs.

The influence of analog length, number of Aib molecules, aromaticity or charge of residues in variable positions, and type of N-terminal protecting groups is discussed as to their influence on potency and efficacy. All eleven Aib IK analogs were active as agonists on both tick and mosquito recombinant receptors, with various potencies (EC_{50}) and binding efficacies on each receptor (Table 2).

3.2. Insect kinin PEG analogs

Five insect kinin analogs incorporating PEG_4 (MS-PEG_4) and PEG_8

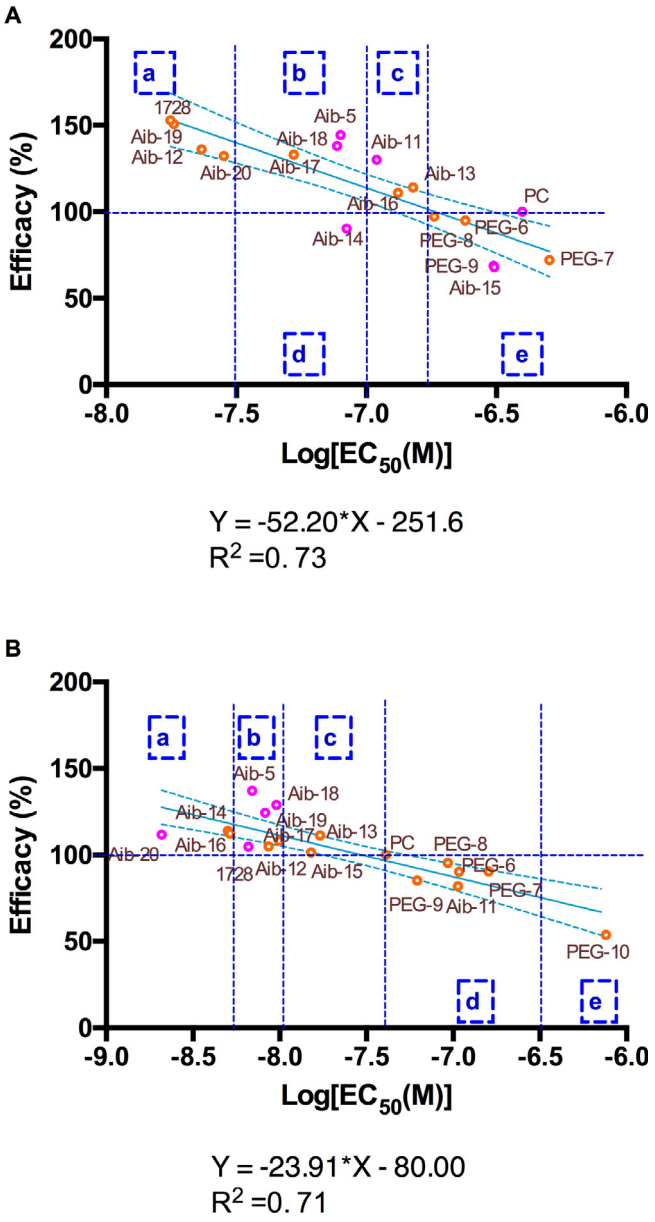

Fig. 3. The correlation between efficacy (efficacy; Y axis) and potency (X axis) of insect kinin (IK) analogs on mosquito (A) and tick (B) kinin receptors. In both figures the X-axis represents Log[EC_{50}(M)] of each analog (Table 2), and the Y axis represents the efficacy (Table 2). The Pearson correlation (two-tailed) analysis was performed independently for the tick and mosquito receptor data sets. The linear regression lines and the 95% confidence intervals (dashed blue lines) were calculated with the "Best-fit value" setting using GraphPad Prism 6.0 (GraphPad Software, La Jolla, CA). The equations for linear regression lines are shown below each graph. Values outside the 95% confidence intervals were considered outliers and are labeled in magenta color. The 18 analogs were separated into different groups based on their physical location on the plot (sector) for each receptor. The plot was divided in sectors as follows: for both mosquito and tick plots, an horizontal line at the efficacy of PC (100%) and the analogs with efficacy > 100% were subsequently divided into three groups (a-c) by EC_{50}. Group (a) was divided by a vertical line for EC_{50} of 30 nM (mosquito receptor) and 5 nM (for tick receptor). Group a represented the most potent analogs that exhibited the same (on mosquito) or higher (on tick) potency as analog 1728 (a highly potent analog). Analogs in group (b) showed the second-highest potency with EC_{50} lower than 100 nM (on mosquito, and are less potent than group a), and with EC_{50} lower than 10 nM (on tick with similar level of potency as 1728). Group (c) represented analogs with intermediate potency in mosquito, with EC_{50s} above the 100 nM line (arbitrarily defined). For tick receptor group (c) included analogs of intermediate potency with EC_{50} between 10 nM and that of the PC = 41 nM (line intercept). The analogs that fell into the lower sector of the plot, relative efficacy < 100% were subdivided as follows: A. For mosquito, there were 2 groups: group (d) on mosquito receptor represented an 'outlier' analog with low efficacy (IK-AIB-14) and (e) which includes all the polyethylene glycol (PEG) modified-analogs. B. For tick, group (d) includes the majority of the PEG analogs and IK-Aib-11, and (e) represented the least potent analogs.

(MS-PEG_8) polymers at the N-terminus were designed, three of which also incorporate the sterically-hindered Aib residue at hydrolysis sites (Table 1 and Fig. 1).

3.3. Activity of Aib analogs on the mosquito kinin receptor

Analogs will be discussed by order of overall activity (Fig. 3A). For the mosquito receptor the first four analogs in Table 2, 1728 (EC_{50} = 17 nM), K-Aib-19 (EC_{50} = 18 nM), IK-Aib-12 (EC_{50} = 23 nM) and IK-Aib-20 (EC_{50} = 28 nM) were significantly more potent than the rest of the analogs (Suppl. Table 1.1, Suppl. Fig. 1A–C), but there were no significant differences among the four, either in potency or efficacy (Table 2; Suppl. Tables 1.1 and 1.2). All four were designed with a blocked N-terminus, Aib or (pyroglutamic acid (pQ)), to impair activity of degrading aminopeptidases, and three of them featured two molecules of Aib (at primary and secondary hydrolysis sites). The sequences only differ in one amino acid at the X^1 position (F, Y and H). Among all 17 analogs tested, IK-AIB-19 was the only analog that had statistically higher efficacy than the PC (Table 2, Suppl. Table 1.2). In the correlation analyses there were no outliers among these four analogs (sector a in Fig. 3A), and although they do not differ in efficacy with respect to the following group of Aib analogs (Fig. 3A, sector b), they have higher potency. For these reasons these are the most desirable IK analogs and candidates to be tested *in vivo*.

After analogs in group *a*, analogs IK-Aib-5, IK-Aib-17, IK-Aib-18 were the most potent group of analogs, with similar EC_{50} values of < 100 nM, significantly more potent than the PC (Table 2, Suppl. Fig. 1A and B, Suppl. Table 1.1). Moreover, their relative activity (bioluminescence) curves completely overlapped (Fig. 2A and B). Although the efficacy was not different from that of the PC at 1 μM (Suppl. Table 1.2), the analogs' curves in Fig. 2(A and B) are shifted to the left, reflecting the significantly higher potency of these analogs with respect to the PC (Suppl. Fig. 1A and B). Besides, the N-terminus of IK-Aib-5 and -18 were further protected from aminopeptidases with an acetyl group and a pyroglutamate, respectively, making them potentially more stable than IK-Aib-17 (Table 2). Importantly, when comparing IK-Aib-17 to IK-Aib-18, the addition of the protective pQ at the N-terminus did not diminish its potency (Table 2, Suppl. Tables 1.1). Correlation analyses grouped them in sector *b* (Fig. 3A), with IK-Aib-5 and IK-Aib-18 being outliers because they had higher efficacy than expected by the regression line.

Notably, IK-Aib-12 (pQ**K**FY[Aib]WGa) in group *a* and IK-Aib-18 (pQ**V**FY[Aib]WGa) in group *b* featured pQ on the N-terminus, and differed only in one residue before the kinin core (Table 3). The EC_{50} value of IK-Aib-12 (23 nM) was significantly lower (3.3-fold) than IK-Aib-18 (77 nM), suggesting a positively charged lysine plays a role in enhancing the analog activity in the presence of pQ on the N-terminus.

Among analogs designed as mono Aib pentapeptides, it appears that there is a higher activity for analogs featuring F or Y over H. Analog IK-Aib-5 (Ac-F**F**[Aib]WG) was significantly more efficacious (higher efficacy) on the receptor than IK-Aib-14 (Ac-F**H**[Aib]WGa), of similar structure (Fig. 2B and C; Suppl. Table 1.2). This resulted in IK-Aib-14 being an outlier in the correlation analyses (Fig. 3A, sector d), despite similar EC_{50}s. Similarly to the above, in unprotected pentapeptides, analog IK-Aib-16 featuring Y (F**Y**[Aib]WGa; EC_{50} = 132 nM) was over 2-fold more potent than analog IK-Aib-15 (F**H**[Aib]WGa;

Table 3
Comparative structure-activity relationships of Aib-analogs based on sequences of aedeskinins on mosquito and tick receptors.

Recombinant mosquito receptor	[Aib]**FF**	[Aib]FY	p**QK**FY	**V**FY	p**QV**FY	Ac-FF	NSKYVSK**QK**FY				
Aedeskinin1 and/or 3[a]		1728	IK-Aib-19	IK-Aib-12	IK-Aib-17	IK-Aib-18	IK-Aib-5	IK-Aib-11	EC50 (nM)	efficacy %	Activity[b]
[Aib]**FF**	1728	–							**17.16**	152.98	Group a
[Aib]FY	IK-Aib-19	ns	–						**18.17**	150.70	Group a
p**QK**FY	IK-Aib-12	ns	ns	–					**23.23**	136.12	Group a
VFY	IK-Aib-17	*	*	*	–				52.63	133.07	Group b
p**QV**FY	IK-Aib-18	*	*	*	ns	–			77.12	138.07	Group b; OL high efficacy
Ac-**FF**	IK-Aib-5	*	*	*	ns	ns	–		78.37	144.35	Group b; OL high efficacy
NSKYVSK**QK**FY	IK-Aib-11	*	*	*	*	ns	ns	–	109.6	130.16	Group c; OL high efficacy
FY	IK-Aib-16	*	*	*	*	ns	ns	ns	132.3	110.84	group c
Aedeskinin2		[Aib]FH IK-Aib-20	Ac-FH IK-Aib-14	NPFH IK-Aib-13	FH IK-Aib-15						
[Aib]FH	IK-Aib-20	–							**28.32**	132.25	Group a
Ac-F**H**	IK-Aib-14	*	–						83.88	**90.17**	Group d; OL low efficacy
NPFH	IK-Aib-13	*	*	–					182	114.10	Group c
FH	IK-Aib-15	*	*	*	–				310.8	**67.85**	Group d; OL low efficacy
Recombinant tick receptor	FY	[Aib]**FF**	Ac-**FF**	p**QV**FY	p**QK**FY	[Aib]FY	**V**FY				
aedeskinin1 and/or 3	IK-Aib-16	1728	IK-Aib-5	IK-Aib-18	IK-Aib-12	IK-Aib-19	IK-Aib-17				
FY	IK-Aib-16	–							**5.17**	112.23	Group a
[Aib]**FF**	1728	ns	–						**6.61**	104.80	Group b; OL low efficacy
Ac-**FF**	IK-Aib-5	ns	ns	–					**6.19**	137.09	Group b; OL high efficacy; above 1728
p**QV**FY	IK-Aib-18	ns	ns	ns	–				**8.24**	124.41	Group b; OL high efficacy; above 1728
p**QK**FY	IK-Aib-12	ns	ns	ns	ns	–			**8.63**	104.88	group b
[Aib]FY	IK-Aib-19	ns	ns	ns	ns	ns	–		**9.56**	128.91	Group b; OL high efficacy; above 1728
VFY	IK-Aib-17	ns	ns	ns	ns	ns	ns	–	**9.93**	108.07	Group b
NSKYVSK**QK**FY	IK-Aib-11	*	*	*	*	*	*	*	106.6	**81.92**	Group d
Aedeskinin2		[Aib]FH IK-Aib-20	Ac-FH IK-Aib-14	FH IK-Aib-15	NPFH IK-Aib-13						
[Aib]FH	IK-Aib-20	–							**2.09**	111.74	Group a; OL low efficacy; above 1728
Ac-FH	IK-Aib-14	ns	–						**5.02**	113.95	Group a; above 1728
FH	IK-Aib-15	*	*	–					15.17	101.49	Group c
NPFH	IK-Aib-13	*	*	ns	–				18.08	111.19	Group c

[a] Only N terminal sequences are shown for clarity; all analogs have the same C-terminus as -[Aib]WGa; for complete sequences see Table 2.
[b] OL stands for outlier in the correlation analyses (Fig. 3), and 'above 1728' means the analog bioluminescence dose-response curve was higher than that of 1728 (Fig. 2E–H). For pair comparisons * = significant differences of potency (EC_{50}; * means $P < 0.05$ by Tukey multiple comparison test) and ns = not significant differences. These are the results of the detailed statistical analyses in Supplementary Tables 1.1 and 2.1.

EC_{50} = 311 nM) (Table 2).

Group *c* consisted of analogs of intermediate potency (Fig. 3A). They showed significant differences with analog(s) in group *b*, while exhibiting significantly greater potency and similar binding efficacies in comparison with the PC (Suppl. Tables 1.1 and 1.2). Their dose-dependent responses were highly similar (Fig. 2A–C) and no statistical difference was detected in either their EC_{50s} (IK-Aib-11,110 nM; IK-Aib-13, 151 nM, and IK-Aib-16,132 nM) or binding efficacies (Table 2; Suppl. Tables 1.1 and 1.2). This group of analogs featured an Aib molecule embedded in full or as a fragment of sequences of aedeskinin 1–3 without any modification on the 2nd hydrolysis site (Table 1), and they are thus expected to be less resistant to hydrolysis by aminopeptidases. Despite its similar potency within group *c*, analog IK-Aib-11 was an outlier above the upper 95% confidence interval for efficacy (Fig. 3A).

It is noteworthy that the pentapeptide IK-Aib-16, FY[Aib]WGa~~,~~ had similar activity to IK-Aib-11 (featuring all 14 residues of aedeskinin 1), as the mosquito kinin receptor preferred hexapeptide kinin analogs over their pentapeptide counterparts in a previous study (Taneja-Bageshwar et al., 2006). Thus, the full sequence of aedeskinin 1 as appears in analog IK-Aib-11 would have been expected to have a greater potency than the corresponding C-terminal pentapeptide analogs. Furthermore, despite its greater length, IK-Aib-11 is less potent than a smaller, similar fragment analog IK-Aib-12 (Table 3).

IK-Aib-19 and IK-Aib-17, hexapeptides with sequences common to aedeskinin 1 and/or aedeskinin 3, showed higher potency than the respective pentapeptide IK-Aib-16 (FY[Aib]WGa) (Table 3, Suppl. Table 1.1). Similarly, for aedeskinin 2 based analogs, IK-Aib-20 and IK-Aib-13 also showed significantly greater potency than the pentapeptide IK-Aib-15 (FH[Aib]WGa) (Fig. 2C, Table 3). IK-Aib-15 had significantly lower potency than all Aib-analogs tested, and in the correlation analyses it was an outlier due to its significantly lower efficacy from groups *a* and *b* (Fig. 3A, Suppl. Table 1.2).

The presence of a mono-Aib group changed the potency of the endogenous aedeskinins. Their rank order of potency was first analog IK-Aib-11 (similar to aedeskinin 1), followed by analog IK-Aib-13 (similar to aedeskinin 2) (Table 2). This is in contrast to the previously determined potencies of the parent peptides, as aedeskinin 2 was found to be more potent on this recombinant receptor than aedeskinin 1 (Pietrantonio et al., 2005).

3.4. Evaluation of Aib analogs on the tick kinin receptor

Evaluation of the Aib IK analog series on the tick recombinant receptor revealed that all retained high potency. The tick receptor is clearly more permissive than the mosquito receptor, as nine of the kinin analogs had potencies at or below 10 nM, two had potencies below 20 nM and only one had EC_{50} above 100 nM (Table 2). All analogs had similar efficacy except for IK-Aib-11, with lower efficacy (Table 2;

Suppl. Table 2.2). In contrast to the mosquito kinin receptor, 1728 was not among the most potent analogs (Table 2; Suppl. Fig. 1E–G), and it is an outlier below the 95% intervals of the regression line (Fig. 3B). Three of the analogs constituted the most potent with an EC_{50} lower than 5 nM and formed group *a*, with no significant differences among them (Table 2; Fig. 3B). The high potency of IK-Aib-20 is particularly noteworthy, with an EC_{50} value of 2 nM, being more potent than 1728 by a factor of 3 and exhibiting a dose-response curve higher than that of 1728 (Fig. 2G), and it was an outlier in the correlation analysis with lower than expected efficacy (Fig. 3). Further, analog IK-Aib-20 was designed based on aedeskinin 2 (features H) (Table 3) and its potency was significantly different from the rest of all analogs except for those in group *a* (Suppl. Table 2.1). Analogs IK-Aib-20 and IK-Aib-14 feature additional protection from aminopeptidase attack (protection that is lacking in IK-Aib-16), and therefore, they are expected to be more biostable. Analog IK-Aib-14 also showed a dose-response curve above the one of 1728 (Fig. 2G).

Analogs with an EC_{50} between 5 and 10 nM were similar in potency (IK-Aib-5, -18, -12, -19, and -17) (Table 2), matched the potency of 1728 and were considered as group *b* (Fig. 3B). This group of IK analogs was designed based on the sequences of aedeskinins 1 and/or 3 (Table 3). Three of them (IK-Aib-5, -18 and -19) showed dose-response curves above that of 1728, and simultaneously were outliers with higher than predicted efficacy in correlation analysis (Fig. 2E–F and 3B). Analogs in group *c*, IK-Aib-15 and IK-Aib-13, were intermediate in potency with a significantly higher EC_{50} that analogs in group *a* (Fig. 3B, Suppl. Table 2.1). These two analogs were designed based on aedeskinin 2 but are not blocked at the N-terminus (Table 3). There is only one analog in group *d* (Fig. 3B), IK-Aib-11, that features 14 residues as in aedeskinin 1, and had the lowest potency and efficacy among all Aib analogs (Table 2, Fig. 2E, Suppl. Table 2).

Within the multi-Aib C-terminal hexapeptide framework, differences in the potency of analogs that feature different aromatic residues (F, Y or H) in variable position 2 of the IK C-terminal pentapeptide core, IK-Aib-20, 1728 and IK-Aib-19 (Table 2), suggest that the tick receptor exhibits a preference for the positively charged, aromatic residue H (IK-Aib-20) (Table 2). In the IK core variable position of the mono-Aib C-terminal pentapeptide framework by contrast, as with the mosquito receptor, the tick receptor exhibits a preference for Y over H, as analog IK-Aib-16 is more potent than IK-Aib-15 by a factor of 3, with this difference being statistically significant.

3.5. Evaluation of PEG analogs on the mosquito kinin receptor

Five insect kinin analogs incorporating PEG_4 [$MS(PEG_4)$] and PEG_8 [$MS(PEG_8)$] polymers, three of which also incorporate the sterically-hindered Aib residue at the core N-terminus, were evaluated on the two recombinant IK receptors. One analog, IK-PEG-10, was not active. As a group, the remaining four PEG analogs had lower potency than the majority of the IK-Aib analogs, with a range of EC_{50}s from 182 nM to 506 nM (Table 2, Suppl. Fig. 1D). They exhibited similar activity as compared with the PC (Suppl. Table 1.2), and in the correlation analyses fell in group *e* (Fig. 3A). The PC was an outlier in the mosquito receptor with a higher efficacy than predicted by the regression line. This may explain that despite having an apparent lower EC_{50}, its dose-response curve closely matches those of IK-PEG-8 and -6. IK-PEG-8, IK-PEG-6 and IK-PEG-9 were similar in potency and the first two are significantly more potent than IK-PEG-7 (Table 2; Suppl. Table 1.1). Further, the overall dose-response curves of IK-PEG-6 and IK-PEG-8 were above the response curves of IK-PEG-7 and IK-PEG-9 (Fig. 2D). IK-PEG-6 and IK-PEG-8, with $MS(PEG_4)$ and $MS(PEG_8)$ groups on the N-terminus, respectively, shared the same amino acid sequence (-RFFPWGa), respectively (Table 1).

Analog IK-PEG-9 fell within the most potent PEG analogs (not different from IK-PEG-8 and -6), however, it is the only one of this group that is also not different from IK-PEG-7, that featured lower potency. The fact that IK-PEG-9 shows similar potency to the first group but also does not differ from IK-PEG-7 can be explained by the shape of the dose-response curve (Fig. 2D): While the efficacy is the same at 1 μM for both analogs, at 10 μM IK-PEG-9 plateaued, behaving as a partial agonist. IK-PEG-7 and IK-PEG-9 have two Aib molecules in the sequence (-R[Aib]FF[Aib]WGa) that can confer additional endopeptidase biostability to the IK sequence, and therefore potentially greater hemolymph residence time when tested *in vivo* than IK-PEG-8 and IK-PEG-10 (-RFFPWGa). Overall, these results revealed that the mosquito kinin receptor did not discriminate PEG analogs with either $MS(PEG_4)$ or $MS(PEG_8)$. The analog IK-PEG-10 ($MS(PEG_8)$-[Aib]FF[Aib]WGa), which is the only analog that lacks the R residue as in IK-PEG-9 ($MS(PEG_8)$-R[Aib]FF[Aib]WGa), is not active on the mosquito receptor. The R may confer an advantage by enhancing solubility properties, by providing a spacer between the IK core region and the PEG polymer, and/or a more favorable ligand receptor interaction due to the presence of the positively charged residue.

3.6. Evaluation of PEG analogs on the tick kinin receptor

The evaluation of IK analogs incorporating PEG polymer attachments at the N-terminus showed that a few (IK-PEG-8 and IK-PEG-9) retained significant activity that matched the potency of the positive control FFFSWGa (Suppl. Fig. 1H, Suppl. Table 2.1). The analog IK-PEG-10, that was not active on the mosquito receptor, was the weakest agonist of all analogs tested on the tick receptor (Table 2; Suppl. Table 2.1). It is the only analog in sector *e* (Fig. 3B), with significant lower potency but comparable efficacy to the other PEG analogs, but lower efficacy than the PC (Suppl. Table 2, Fig. 2H). The remaining four PEG analogs as a group, had lower activity than the majority of the IK-Aib analogs, with an EC_{50} range from 62 nM to 160 nM (Table 2, Suppl. Fig. 1D), and are placed in group *d* (Fig. 3B).

The Aib-containing analog IK-PEG-9 exhibited the greatest potency among this IK-PEG series on the tick receptor with an EC_{50} of 62 nM. IK-PEG-9 (featuring $MS(PEG_8)$, was significantly more potent than its' P_4 counterpart IK-PEG-7 ($MS(PEG_4)$-R[Aib]FF[Aib]WGa) with EC_{50} of 160 nM (Table 2). These are the only two that exhibited significant differences in potency (Suppl. Table 2.1) among the four active PEG analogs featuring overall similar dose-response curves (Fig. 2H). Therefore, for PEG analogs containing Aib, the tick receptor reveals a preference for the longer $MS(PEG_8)$ polymer over the $MS(PEG_4)$ polymer. The two Aib residues of these two analogs confer enhanced resistance to endopeptidase hydrolysis, potentially increasing *in vivo* hemolymph residence time.

While IK-PEG-10 retains some activity on the tick receptor, it was inactive on the mosquito receptor, reinforcing the fact that the recombinant tick receptor cell line is more responsive to ligand binding than the mosquito receptor cell line. Of striking significance, however, is the contrast between the most potent PEG analog IK-PEG-9 ($MS(PEG_8)$-R[Aib]FF[Aib]WGa) and the least potent, IK-PEG-10 ($MS(PEG_8)$-[Aib]FF[Aib]WGa). The only difference between these two IK-PEG analogs is the presence of an R residue in the former (Table 2). The arginine (R) residue in the more active PEG analogs containing Aib proved to be an important component for activity on both invertebrate receptors. The R (arg) may confer an advantage by enhancing solubility properties, by providing a spacer between the IK core region and the PEG polymer, and/or a more favorable ligand receptor interaction.

4. Summary and conclusions

The evaluation of a series of IK-Aib analogs incorporating sequences of endogenous aedeskinins from the *Ae. aegypti* mosquito on two invertebrate receptor cell lines revealed a number of highly potent biostable IK mimics. To prevent hydrolysis by aminopeptidases biostable IK analogs incorporating a second Aib residue N-terminal to Phe^1 of the core were synthesized. On the mosquito *Ae. aegypti* kinin receptor three

highly potent, biostable Aib analogs (group *a*) matched the activity of IK analog 1728, that has previously demonstrated insect disruptive and/or aversive activity; therefore it is possible these analogs may have similarly desirable activity. They may also be useful tools in further defining the structural characteristics required to induce aversive and/or deterrent behavior in the mosquito and kissing bug. Evaluation of analogs with PEG polymers attached on the N-terminus revealed certain analogs with similar or higher potency as the positive control peptide, and they are important tools for testing kinin activities *in vivo*.

The most active of the Aib and PEG analogs identified in this study represent new tools for arthropod endocrinologists studying insect kinin regulated processes, particularly in ticks for which a role for the insect kinins has yet to be established. The potent, biostable analogs presented here would demonstrate longer hemolymph residence times, making them particularly suitable for the study of *in vivo* physiological and behavioral effects of kinin neuropeptides. Furthermore, these analogs, either in isolation or in combination with biostable analogs of other neuropeptide classes that also regulate aspects of diuretic, antidiuretic, digestive, reproductive and/or developmental processes, represent potential leads in the development of selective, environmentally friendly pest arthropod control agents capable of disrupting those critical processes.

Acknowledgements

RJN received support from the US Department of Agriculture/Department of Defense Deployed War Fighter Protection Initiative 6202-22000-029-00D. We thank Allison Strey (USDA) for able technical assistance in the synthesis, purification and characterization of the peptide analogs. Research in PVP laboratory was supported by USDA-NIFA-AFRI Foundational Grant number 2016-67015-24918 (Animal Health and Well-Being), and by a Vector Biology seed grant from Texas A&M AgriLife Research. C. Xiong is a Ph.D. student in the Entomology graduate program. Drs. Daeweon Lee and Christina Brock are acknowledged for technical assistance for cell assays.

Appendix A. Supplementary data

Supplementary data associated with this article can be found, in the online version, at https://doi.org/10.1016/j.ygcen.2018.08.002.

References

Boccù, E., Velo, G., Veronese, F., 1982. Pharmacokinetic properties of polyethylene glycol derivatized superoxide dismutase. Pharmacol. Res. Commun. 14, 113–120.
Coast, G., 2007. The endocrine control of salt balance in insects. Gen. Comp. Endocrinol. 152, 332–338.
Coast, G.M., Holman, G.M., Nachman, R.J., 1990. The diuretic activity of a series of cephalomyotropic neuropeptides, the achetakinins, on isolated Malpighian tubules of the house cricket, *Acheta domesticus*. J. Insect Physiol. 36, 481–488.
Coast, G.M., Orchard, I., Phillips, J.E., Schooley, D.A., 2002. Insect diuretic and antidiuretic hormones. Adv. Insect Physiol. 29, 279–409.
Cornell, M.J., Williams, T.A., Lamango, N.S., Coates, D., Corvol, P., Soubrier, F., Hoheisel, J., Lehrach, H., Isaac, R.E., 1995. Cloning and expression of an evolutionary conserved single-domain angiotensin converting enzyme from *Drosophila melanogaster*. J. Biol. Chem. 270, 13613–13619.
De Loof, A., 2008. Ecdysteroids, juvenile hormone and insect neuropeptides: recent successes and remaining major challenges. Gen. Comp. Endocrinol. 155, 3–13.
Gäde, G., 2004. Regulation of intermediary metabolism and water balance of insects by neuropeptides. Ann. Rev. Entomol. 49, 93–113.
Gäde, G., Goldsworthy, G.J., 2003. Insect peptide hormones: a selective review of their physiology and potential application for pest control. Pest Manage. Sci. 59, 1063–1075.
Harshini, S., Manchu, V., Sunitha, V., Sreekumar, S., Nachman, R., 2003. In vitro release of amylase by culekinins in two insects: *Opsinia arenosella* (Lepidoptera) and *Rhynchophorus ferrugineus* (Coleoptera). Trends Life Sci. 17, 61–64.
Holman, G.M., Nachman, R., Wright, M., 1990. Insect neuropeptides. Annu. Rev. Entomol. 35, 201–217.
Holman, G.M., Nachman, R.J., Coast, G.M., 1999. Isolation, characterization and biological activity of a diuretic myokinin neuropeptide from the housefly, *Musca domestica*. Peptides 20, 1–10.
Holmes, S., Barhoumi, R., Nachman, R., Pietrantonio, P.V., 2003. Functional analysis of a G protein-coupled receptor from the Southern cattle tick *Boophilus microplus* (Acari: Ixodidae) identifies it as the first arthropod myokinin receptor. Insect Mol. Biol. 12, 27–38.
Holmes, S., He, H., Chen, A., Ivie, G., Pietrantonio, P.V., 2000. Cloning and transcriptional expression of a leucokinin-like peptide receptor from the Southern cattle tick, *Boophilus microplus* (Acari: Ixodidae). Insect Mol. Biol. 9, 457–465.
Jeffers, L.A., Roe, R.M., 2008. The movement of proteins across the insect and tick digestive system. J. Insect Physiol. 54, 319–332.
Kersch, C.N., Pietrantonio, P.V., 2011. Mosquito *Aedes aegypti* (L.) leucokinin receptor is critical for *in vivo* fluid excretion post blood feeding. FEBS Lett. 585, 3507–3512.
Kim, D.-H., Kim, Y.-J., Adams, M.E., 2018. Endocrine regulation of airway clearance in *Drosophila*. Proc. Natl. Acad. Sci. 115, 1535–1540.
Kwon, H., Agha, M.A., Smith, R.C., Nachman, R.J., Marion-Poll, F., Pietrantonio, P.V., 2016. Leucokinin mimetic elicits aversive behavior in mosquito *Aedes aegypti* (L.) and inhibits the sugar taste neuron. Proc. Natl. Acad. Sci. 113, 6880–6885.
Lamango, N.S., Sajid, M., Isaac, R.E., 1996. The endopeptidase activity and the activation by Cl-of angiotensin-converting enzyme is evolutionarily conserved: purification and properties of an angiotensin-converting enzyme from the housefly, *Musca domestica*. Biochem. J. 314, 639.
Lu, H.L., Kersch, C., Pietrantonio, P.V., 2011a. The kinin receptor is expressed in the Malpighian tubule stellate cells in the mosquito *Aedes aegypti* (L.): a new model needed to explain ion transport? Insect Biochem. Mol. Biol. 41, 135–140.
Lu, H.L., Kersch, C.N., Taneja-Bageshwar, S., Pietrantonio, P.V., 2011b. A calcium bioluminescence assay for functional analysis of mosquito (*Aedes aegypti*) and tick (*Rhipicephalus microplus*) G protein-coupled receptors. Jove-J. Vis. Exp. 50 e273210.273791/272732.
Nachman, R.J., Coast, G.M., Douat, C., Fehrentz, J.-A., Kaczmarek, K., Zabrocki, J., Pryor, N.W., Martinez, J., 2003. A C-terminal aldehyde insect kinin analog enhances inhibition of weight gain and induces significant mortality in *Helicoverpa zea* larvae. Peptides 24, 1615–1621.
Nachman, R.J., Coast, G.M., Holman, G.M., Beier, R.C., 1995. Diuretic activity of C-terminal group analogues of the insect kinins in *Acheta domesticus*. Peptides 16, 809–813.
Nachman, R.J., Holman, G.M., 1991. Myotropic insect neuropeptide families from the cockroach *Leucophaea maderae*: structure—activity relationships. In: Menn, J.J., Masler, Edward P. (Eds.), Insect Neuropeptides: Chemistry, Biology, and Action. American Chemical Society, Washington, D.C., pp. 194–214.
Nachman, R.J., Isaac, R.E., Coast, G.M., Holman, G.M., 1997a. Aib-containing analogues of the insect kinin neuropeptide family demonstrate resistance to an insect angiotensin-converting enzyme and potent diuretic activity. Peptides 18, 53–57.
Nachman, R.J., Isaac, R.E., Coast, G.M., Roberts, V.A., Lange, A.B., Orchard, I., Holman, G.M., Teal, P.E., 1997b. Active conformation and mimetic analog development for the Pyrokinin—PBAN—Diapause—Pupariation and Myosuppressin insect neuropeptide families. In: Hedin, P.A., Hollingworth, R.M., Masler, E.P., Miyamoto, J., Thompson, D.G. (Eds.), Phytochemicals for Pest Control. American Chemical Society, Washington, DC, pp. 277–291.
Nachman, R.J., Roberts, V.A., Holman, G.M., Trainer, J., 1990. Concensus chemistry and conformation of an insect neuropeptide family analogous to tachykinins. Prog. Clin. Biol. Res. 342, 60.
Nachman, R.J., Strey, A., Isaac, E., Pryor, N., Lopez, J.D., Deng, J.-G., Coast, G.M., 2002. Enhanced in vivo activity of peptidase-resistant analogs of the insect kinin neuropeptide family. Peptides 23, 735–745.
Nachman, R.J., Tilley, J.W., Hayes, T.K., Holman, G.M., Beier, R.C., 1994. Pseudopeptide mimetic analogs of insect neuropeptides. In: Hedin, P., Menn, J.J., Hollingworth, R.M. (Eds.), Natural and Engineered Pest Management Agents. American Chemical Society, Washington DC, pp. 210–229.
Nässel, D.R., 2002. Neuropeptides in the nervous system of *Drosophila* and other insects: multiple roles as neuromodulators and neurohormones. Prog. Neurobiol. 68, 1–84.
Pietrantonio, P.V., Jagge, C., Taneja-Bageshwar, S., Nachman, R., Barhoumi, R., 2005. The mosquito *Aedes aegypti* (L.) leucokinin receptor is a multiligand receptor for the three Aedes kinins. Insect Mol. Biol. 14, 55–67.
Predel, R., Kellner, R., Rapus, J., Penzlin, H., Gáde, G., 1997. Isolation and structural elucidation of eight kinins from the retrocerebral complex of the American cockroach, *Periplaneta americana*. Regul. Pept. 71, 199–205.
Roberts, V.A., Nachman, R.J., Coast, G.M., Hariharan, M., Chung, J.S., Holman, G.M., Williams, H., Tainer, J.A., 1997. Consensus chemistry and R-turn conformation of the active core of the insect kinin neuropeptide family. Chem. Biol. 4, 105–117.
Seinsche, A., Dyker, H., Lösel, P., Backhaus, D., Scherkenbeck, J., 2000. Effect of helicokinins and ACE inhibitors on water balance and development of *Heliothis virescens* larvae. J. Insect Physiol. 46, 1423–1431.
Shen, H., Brandt, A., Witting-Bissinger, B.E., Gunnoe, T.B., Roe, R.M., 2009. Novel insecticide polymer chemistry to reduce the enzymatic digestion of a protein pesticide, trypsin modulating oostatic factor (TMOF). Pest. Biochem. Physiol. 93, 144–152.
Taneja-Bageshwar, S., Strey, A., Isaac, R.E., Coast, G.M., Zubrzak, P., Pietrantonio, P.V., Nachman, R.J., 2009. Biostable agonists that match or exceed activity of native insect kinins on recombinant arthropod GPCRs. Gen. Comp. Endocrinol. 162, 122–128.
Taneja-Bageshwar, S., Strey, A., Zubrzak, P., Williams, H., Reyes-Rangel, G., Juaristi, E., Pietrantonio, P., Nachman, R.J., 2008. Identification of selective and non-selective, biostable β-amino acid agonists of recombinant insect kinin receptors from the southern cattle tick *Boophilus microplus* and mosquito *Aedes aegypti*. Peptides 29, 302–309.
Taneja-Bageshwar, S., Strey, A., Zubrzak, P., Pietrantonio, P.V., Nachman, R.J., 2006. Comparative structure-activity analysis of insect kinin core analogs on recombinant kinin receptors from Southern cattle tick *Boophilus microplus* (Acari: Ixodidae) and mosquito *Aedes aegypti* (Diptera: Culicidae). Arch. Insect Biochem. Physiol. 62, 128–140.
Torfs, P., Nieto, J., Veelaert, D., Boon, D., Water, G., Waelkens, E., Derua, R., Calderon, J., Loof, A., Schoofs, L., 1999. The kinin peptide family in invertebrates. Ann. N. Y. Acad. Sci. 897, 361–373.
Veenstra, J.A., Pattillo, J.M., Petzel, D.H., 1997. A single cDNA encodes all three *Aedes* leucokinins, which stimulate both fluid secretion by the Malpighian tubules and hindgut contractions. J. Biol. Chem. 272, 10402–10407.